

# Coulomb Log for Conductivity of Dense Plasmas

C. E. Starrett<sup>1,\*</sup>

<sup>1</sup>*Los Alamos National Laboratory, P.O. Box 1663, Los Alamos, NM 87545, U.S.A.*

(Dated: August 23, 2018)

The Coulomb log ( $\log \Lambda$ ) approximation is widely used to approximate electron transport coefficients in dense plasmas. It is a classical approximation to the momentum transport cross section. The accuracy of this approximation for electrical conductivity in dense plasmas is assessed by comparing to fully quantum mechanical calculations for realistic scattering potentials. It is found that the classical approximation is accurate to  $\pm 10\%$  when  $\log \Lambda > 3$ , irrespective of the plasma species. The thermodynamic regime (density and temperature) for which  $\log \Lambda > 3$  corresponds to does, however, strongly depend on the material. For increasing  $Z$ ,  $\log \Lambda$  is greater than 3 for increasingly high temperatures and lower densities.

Keywords: Electrical conductivity, dense plasmas, Coulomb Log

## I. INTRODUCTION

The Coulomb Log is a widely used concept in low density plasma physics that allows rapid calculation of the electron-ion momentum transport cross section [1]. It is used to calculate electron and ion transport coefficients. The core approximation is that Rutherford's classical cross section is assumed, but with physically motivated impact parameter cut-offs to guarantee finite results. It is also used for modeling dense plasmas that are found in neutron and white dwarf stars [2, 3], for modeling Inertial Confinement Fusion [4, 5], and for studying temperature equilibration [6–9] and stopping power [10, 11].

The dense plasma environment raises questions about the validity of the core approximation: the classical Rutherford cross section. This neglects electron screening (polarization), core-valence orthogonality, and ion correlations; effects that are known to be important when modeling dense plasmas. Authors typically use the impact parameter cut-offs to account for plasma effects such as degeneracy, ion-correlations and electron screening [12–14]. However, such *ad hoc* corrections must be tested. The accuracy of the Coulomb Log relative to quantum calculations that assume a Debye screening potential has been tested [6], as has the effect of ion-ion correlations again assuming a Debye interaction [14].

In this work the accuracy of the Coulomb Log approach in dense plasmas is assessed through comparison with fully quantum mechanical calculations for a scattering potential that realistically accounts for all the above mentioned physics. This potential is the so-called potential of mean force [15]. It is based on density functional theory (DFT) [16] and the quantum Ornstein Zernike equations [17]. Recently it was shown that calculations of the electrical conductivity using this potential agreed well with existing experiments and with multi-center DFT MD (molecular dynamics) calculations based on the Kubo-Greenwood formula [15]. Hence, through a

comparison of electrical conductivity resulting from the mean force and Coulomb Log approaches the accuracy of the latter is assessed.

In this work, the accuracy of the Coulomb log approach is assessed as a function of plasma conditions and make-up (temperature, density and nuclear charge). Plasmas of pure hydrogen, beryllium, aluminum, copper, silver and lutetium are considered, and plasma conditions from 10 eV through 1 keV are covered. The relationship between the value of the Coulomb log and its accuracy is also tested for these plasmas. Since the Classical Coulomb log method relies on an input of the average ionization, a simple and widely used model for estimating the average ionization (the Thomas-Fermi Cell model [18]) is also tested.

## II. THEORY

### A. The Coulomb Log approximation

The non-relativistic quantum mechanical expression for the momentum transport cross section is

$$\sigma_{TR}(\epsilon) = \frac{4\pi}{p^2} \sum_{l=0}^{\infty} (l+1) (\sin(\eta_{l+1} - \eta_l))^2 \quad (1)$$

where the  $\eta_l = \eta_l(\epsilon)$  are the scattering phase shifts,  $\epsilon$  is the electron energy and  $p$  its momentum. The sum over orbital angular momentum quantum number  $l$ , while formally to  $\infty$  does converge for finite  $\epsilon$ , since the phase shifts approach zero for large  $l$ . For classical electrons the momentum transport cross section is [11]

$$\sigma_{TR}(\epsilon) = \frac{4\pi \bar{Z}^2 e^2}{p^4} \log \Lambda \quad (2)$$

where the average ionization of the plasma is  $\bar{Z} = \bar{n}_e^0/n_i^0$  ( $\bar{n}_e^0$  is the average ionized electron number density,  $n_i^0$  the number density of nuclei).  $\log \Lambda$  is the so-called coulomb log [12, 19, 20]

$$\log \Lambda = \frac{1}{2} \log(1 + b_{max}^2/b_{min}^2) \quad (3)$$

\*Electronic address: starrett@lanl.gov

This arises from consideration of Coulomb collisions, assuming Rutherford cross section and small angle scattering, with  $b_{min}$  and  $b_{max}$  being the assumed minimum and maximum impact parameters.

$b_{max}$  is assumed to be [12]

$$b_{max} = \max(\lambda_{DH}, R) \quad (4)$$

where  $R$  is the ion sphere radius and  $\lambda_{DH}$  is the degeneracy corrected Debye-Hückel screening length

$$\lambda_{DH}^{-2} = \frac{4\pi\bar{n}_e^0 e^2}{k(T^2 + T_F^2)^{\frac{1}{2}}} + \frac{4\pi\bar{Z}^2 n_i^0 e^2}{kT} \quad (5)$$

where  $T$  is the temperature and  $T_F$  is the Fermi temperature.  $b_{min}$  is assumed to be [12]

$$b_{min} = \max(\lambda_{dB}, b_{\perp}) \quad (6)$$

where  $\lambda_{dB}$  is the de Broglie wave length

$$\lambda_{dB} = \frac{\hbar}{2m\bar{v}} \quad (7)$$

and  $b_{\perp}$  is the classical closest distance of approach

$$b_{\perp} = \frac{\bar{Z}e^2}{m\bar{v}^2} \quad (8)$$

Here  $\bar{v}$  is taken to be

$$\bar{v} = \max(v_{rms}, v_F) \quad (9)$$

where  $v_{rms} = \sqrt{3kT/m}$ , where  $T$  is the temperature, is the root mean squared velocity and  $v_F$  is the Fermi velocity.

It is also possible to evaluate the momentum transport cross section in Born approximation, which is quantum mechanical, but is only correct in the high electron-energy limit

$$\sigma_{TR}^{Born}(\epsilon) = \frac{\pi}{p^2} \int_0^{2p} dq q^3 \left| \frac{V(q)}{2\pi} \right| \quad (10)$$

where  $V(q)$  is the scattering potential. If  $V(r)$  is assumed to be a Debye potential then the Born result becomes

$$\sigma_{TR}^B(\epsilon) = \frac{4\pi\bar{Z}^2 e^2}{p^4} \log \Lambda^B \quad (11)$$

where

$$\log \Lambda^B = \frac{1}{2} \left( \log \left( 1 + \frac{b_{max}^2}{b_{min}^2} \right) - \frac{(b_{max}/b_{min})^2}{1 + (b_{max}/b_{min})^2} \right) \quad (12)$$

where  $b_{max} = \lambda_{DH}$  and  $b_{min} = \lambda_{dB}$ . For the Born approximation the form of  $b_{max}$  and  $b_{min}$  are not assumed, as they are in the classical case, but derived. However, one can view equation (12) as a quantum correction to the classical formula (3), and use equations (6) and (4) for  $b_{min}$  and  $b_{max}$ .

In the results section calculations using equations (1), (2) and (11) are compared using equations (6) and (4) in the classical and Born approximations.

## B. Conductivity Model

In the relaxation time approximation, or Krook model [21, 22], the dc conductivity is given by

$$\sigma_{DC} = \frac{1}{3\pi^2} \int_0^{\infty} \left( -\frac{df(\epsilon, \mu)}{d\epsilon} \right) v^3 \tau_{\epsilon} d\epsilon \quad (13)$$

where  $f(\epsilon, \mu)$  is the Fermi-Dirac occupation factor,  $\epsilon$  the electron energy  $\epsilon = mv^2/2$ ,  $\mu$  is the electron chemical potential and  $\tau_{\epsilon}$  is the relaxation time. This last is related to the electron-ion momentum transport cross section  $\sigma_{TR}(\epsilon)$

$$\tau_{\epsilon} = \frac{1}{n_i^0 v \sigma_{TR}(\epsilon)} \quad (14)$$

The model, equation (13), ignores the effect of electron-electron collisions. These can be taken into account, for example using the method of reference [23]. Since our aim here is to assess the accuracy of the Coulomb logarithm approach that approximates the electron-ion cross section, it is safe to ignore electron-electron collisions, with the understanding that if the actual conductivity is required, for example, to compare with experiment, then this effect must be accounted for.

## C. Potential of Mean Force Model

The potential of mean force  $V^{MF}(r)$  for conductivity calculations was introduced in reference [15] in analogy with the well known classical potential of mean force. It is given by

$$\begin{aligned} V^{MF}(r) = & V_{ie}(r) + n_i^0 \int d^3r' \frac{C_{ie}(|\mathbf{r} - \mathbf{r}'|)}{-\beta} h_{ii}(r') \\ & + \bar{n}_e^0 \int d^3r' \frac{C_{ee}(|\mathbf{r} - \mathbf{r}'|)}{-\beta} h_{ie}(r') \end{aligned} \quad (15)$$

where  $V_{ie}(r)$  is the electron-ion interaction potential, including a nuclear Coulomb term and the Coulombic and exchange electron interaction terms,  $C_{ie}(r)$  ( $C_{ee}(r)$ ) is the electron-ion (electron-electron) direct correlation function, and  $\beta = 1/kT$ , where  $T$  is the temperature.

The accuracy of conductivity calculations based on this potential was assessed in reference [15]. It was found to be in generally good agreement with available experiments, as well as with DFT-MD and Quantum Lenard-Balescu calculations [24]. It was shown to be less reliable in the metal to insulator transition region at low temperature. In this work, the focus is on regimes far from this region, i.e. at higher temperatures.

The potential is calculated using a DFT based average atom model coupled to the quantum Ornstein-Zernike equations [25, 26]. This model is well tested and accurate in the dense plasma regime [27–29]. Note that this model

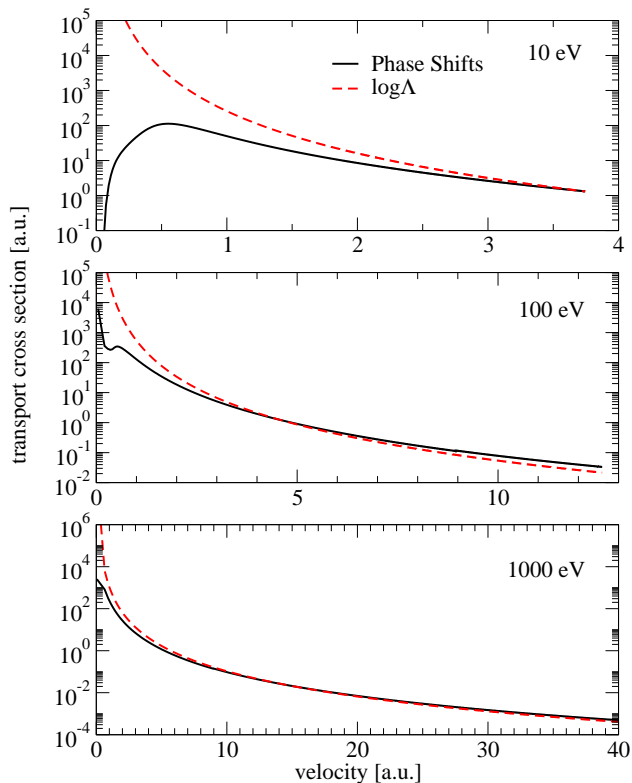


FIG. 1: (Color online) Momentum transport cross sections for beryllium at  $0.185 \text{ g/cm}^3$ .

also provides the average ionization  $\bar{Z} = \bar{n}_e^0/n_i^0$ , from which  $\mu$  is known. The temperature dependent exchange and correlation potential of reference [30] has been used in all our calculations.

An important modelling assumption is that the conductivity can be calculated assuming that the plasma is made up of an ensemble of identical pseudo-atoms, each with an ionization equal to the average ionization of the plasma ( $\bar{Z}$ ). This latter is determined within the model [26]. In reality the plasma is composed of a distribution of ions with different electronic structures. This single-average-ionization assumption is not tested here, but it is noted that this assumption is also used in the classical coulomb log approach, so a comparison is meaningful.

### III. RESULTS

The classical model for  $\sigma_{TR}$  described in section II A is identical to widely used Lee-More model (LM) [12]. LM

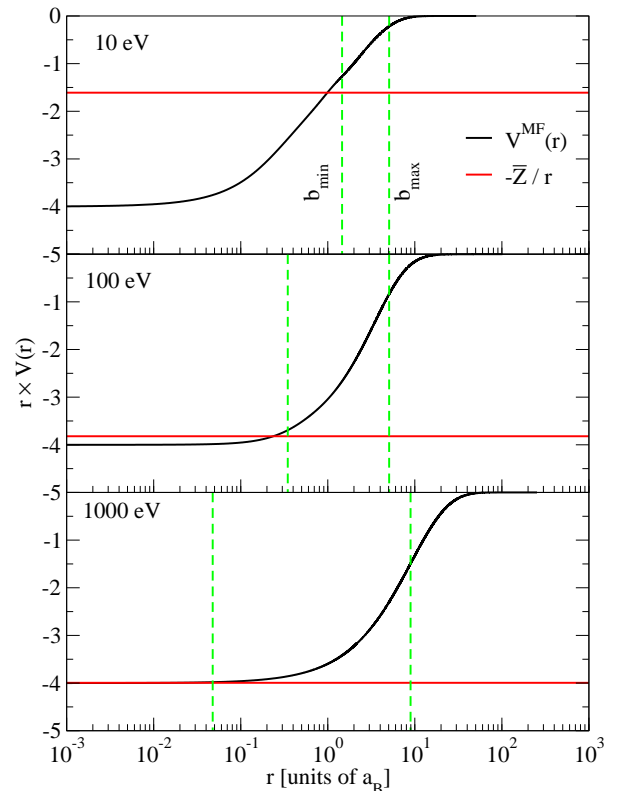


FIG. 2: (Color online) Scattering potentials for beryllium at  $0.185 \text{ g/cm}^3$ .

also introduce a minimum allowed value for  $\log \Lambda$  of  $2.0$ <sup>1</sup>. Desjarlais [31] built on and improved upon the LM model to make it more accurate for metal-insulator transitions, a regime not considered here.

In figure 1 the momentum transport cross section for beryllium at  $1/10^{th}$  of solid density for 10, 100 and 1000 eV is shown. The fully quantum mechanical calculation (labeled “Phase Shifts”) is compared to the classical result (labeled “log  $\Lambda$ ”). The range of velocities shown for each temperature is restricted to the region where  $\sigma_{TR}$  contributed appreciably to the integral in equation (13).

At 1000 eV the quantum and classical transport cross sections are close due to the high energies of the electrons. For small electron velocities the results diverge as the quantum result is finite, while the classical cross section scales as  $\sim v^{-3}$ . For  $kT = 100 \text{ eV}$ , the results are again similar. But for  $kT = 10 \text{ eV}$ , there is a very significant difference. Clearly this is due to the enhanced importance of low energy electrons relative to the higher temperature cases.

<sup>1</sup> LM also used a separate model for for solids, a region of phase space not encountered in this work.

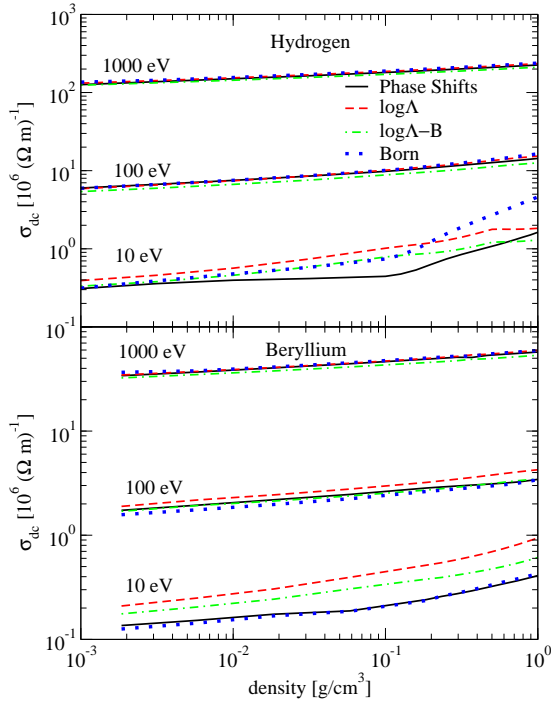


FIG. 3: (Color online) Electron-ion electrical conductivity of hydrogen and beryllium.

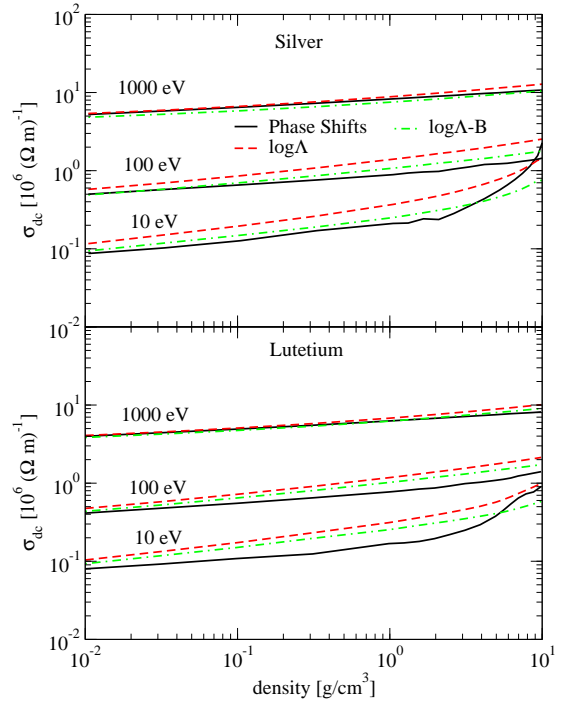


FIG. 5: (Color online) Electron-ion electrical conductivity of silver and lutetium.

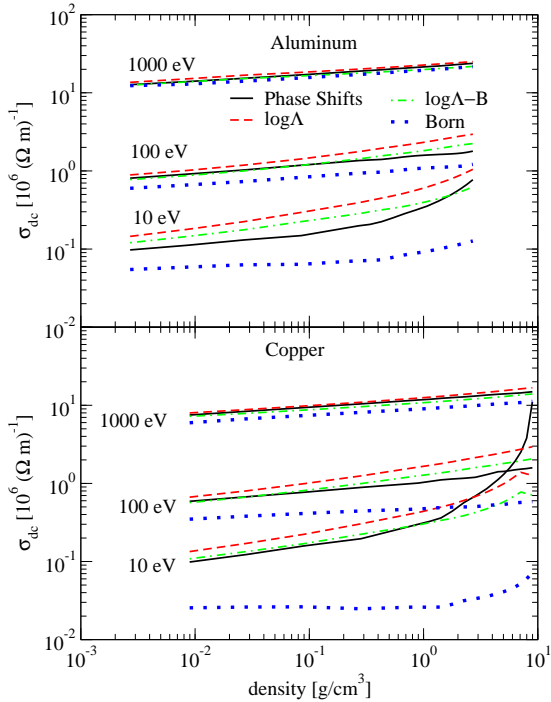


FIG. 4: (Color online) Electron-ion electrical conductivity of aluminum and copper.

For the same plasmas as in figure 1, in figure 2 the scattering potentials are shown. In the classical case, the Rutherford Cross section is for a purely Coulombic potential  $-\bar{Z}/r$ . For the quantum case, where  $V^{MF}(r)$  is used, the potential is screened (i.e. short ranged) and  $V^{MF}(r) \rightarrow -Z/r$  as  $r \rightarrow 0$ , where  $Z$  is the nuclear charge. Also shown in the figure are  $b_{min}$  and  $b_{max}$  for each case. Clearly the proximity of the transport cross sections in figure 1 is not due to the similarity of the scattering potentials, but rather the nearly free electron character of the high energy electrons.

In figures 3 to 5 the electrical conductivity of hydrogen, beryllium, aluminum, copper, silver and lutetium plasmas is shown. The range of densities considered is  $1/1000^{th}$  of normal (i.e solid) to normal density. For hydrogen  $0.001$  to  $1$   $g/cm^3$  is used. The results shown in these plots include fully quantum (“Phase Shifts”), classical (“log  $\Lambda$ ”), classical but with the Born correction (“log  $\Lambda - B$ ”) and quantum Born (“Born”) that uses equation (10).

The trends are clear; for “Born”, agreement with the quantum calculation is reasonable for low  $Z$  (H and Be), but becomes poor for mid  $Z$  (Al and Cu). For high  $Z$  (Ag and Lu) the Born result is not shown as it is in so poor agreement that the figure becomes hard to read. The Born approximation assumes that the scattered electron wave function is a plane wave, i.e. a free state. Clearly the stronger the scatterer, the worse the Born approxi-

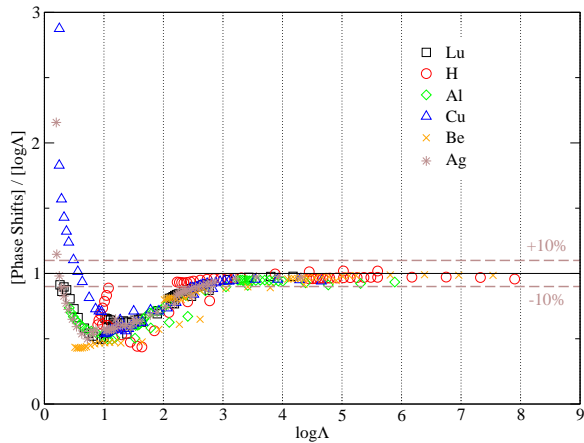


FIG. 6: (Color online) The ratio of the full quantum calculation to the classical  $\log \Lambda$  approach.

mation will be, as borne out by the results. Generally speaking, the Born cross section overestimates the cross section. Here that translates to a larger transport cross section, a shorter relaxation time and therefore a reduced conductivity.

For “ $\log \Lambda$ ” and “ $\log \Lambda - B$ ” generally excellent agreement with the quantum calculation is seen at  $kT = 1000$  eV. The Born correction sometime makes agreement better, and sometimes worse, though the effect is small. At  $kT = 100$  eV, for low  $Z$  agreement with the quantum calculation is good, but becomes poorer as  $Z$  is increased. The Born correction mostly improves the results, but not universally. At  $kT = 10$  eV, agreement of both the  $\log \Lambda$  approaches with the fully quantum results is generally relatively poor.

That the Born correction typically (but not universally) improves agreement with the quantum results is *prima facie* surprising, given how poor the quantum Born approximation does, in contrast to the classical “ $\log \Lambda$ ”. However, the classical cross section without the ad hoc impact parameter cut off’s would yield an infinite cross section and therefore zero conductivity everywhere. Hence it is reasonable that the Born correction could improve agreement.

The value of the Coulomb Log is sometimes used as a metric for the validity of the approximation itself. For example, LM allow a minimum value of  $\log \Lambda = 2.0$ . In figure 6 the value of  $\log \Lambda$  is plotted against the ratio of the quantum result to the classical result (without the Born correction). The results correspond to all cases considered in figures 3 to 5, for the full range of densities and temperatures. An interesting behavior is observed; for all materials considered a similar trend in accuracy is seen. This semi-universal behavior suggests the inaccuracy of the classical method is caused by the same physics, irrespective of the material, and perhaps that the classical

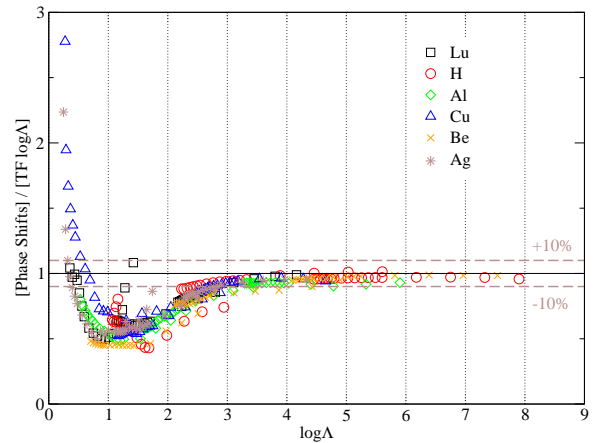


FIG. 7: (Color online) As in figure 6 but with the ionization for the classical  $\log \Lambda$  method determined using the Thomas-Fermi cell model [18].

approximation could be further improved, though this is not attempted here.

For  $\log \Lambda > 3$  the classical method is accurate to  $\pm 10\%$ . This confirms the use of  $\log \Lambda$  as a indicator of accuracy. For  $\log \Lambda \approx 2$  the error is  $\sim 50\%$ . For smaller values of  $\log \Lambda$  there first appears a crossing point, then the classical method grossly underestimates the quantum result.

The classical  $\log \Lambda$  approach depends on knowledge of the average ionization  $\bar{Z}$ . For figures 3 to 6 this was determined using the same model as was used to generate the potential  $V^{MF}$ . This is a quantum mechanical DFT based model that takes a few minutes per density and temperature point to run. A much faster and more widely used model is the Thomas-Fermi cell (TFC) model [18]. This model is used extensively to give a quick estimate of the plasma equation of state and ionization. It is very computationally stable and efficient, taking only a fraction of a second to return a result. The price of this speed is physical accuracy.

In figure 7 the full quantum results are compared with the classical  $\log \Lambda$  method using the TFC model for  $\bar{Z}$ . Different options are available for the ionization definition using the TFC model [32]. We have used the electron density at the edge of the cell, which is equal to the electron density in zero potential with a chemical potential determined by the model. Somewhat surprisingly, the comparison in figure 7 shows that the TFC ionization gives similar agreement to using  $\bar{Z}$  from the full quantum calculation as seen in figure 6. This can be explained by the relatively high temperatures considered here (10, 100 and 1000 eV), where the TFC model is more accurate. This is a useful result. It means that for  $\log \Lambda > 3$  the TFC model can be used to rapidly estimate the DC conductivity of dense plasmas to  $\pm 10\%$  accuracy.

What region of phase space does  $\log \Lambda > 3$  correspond

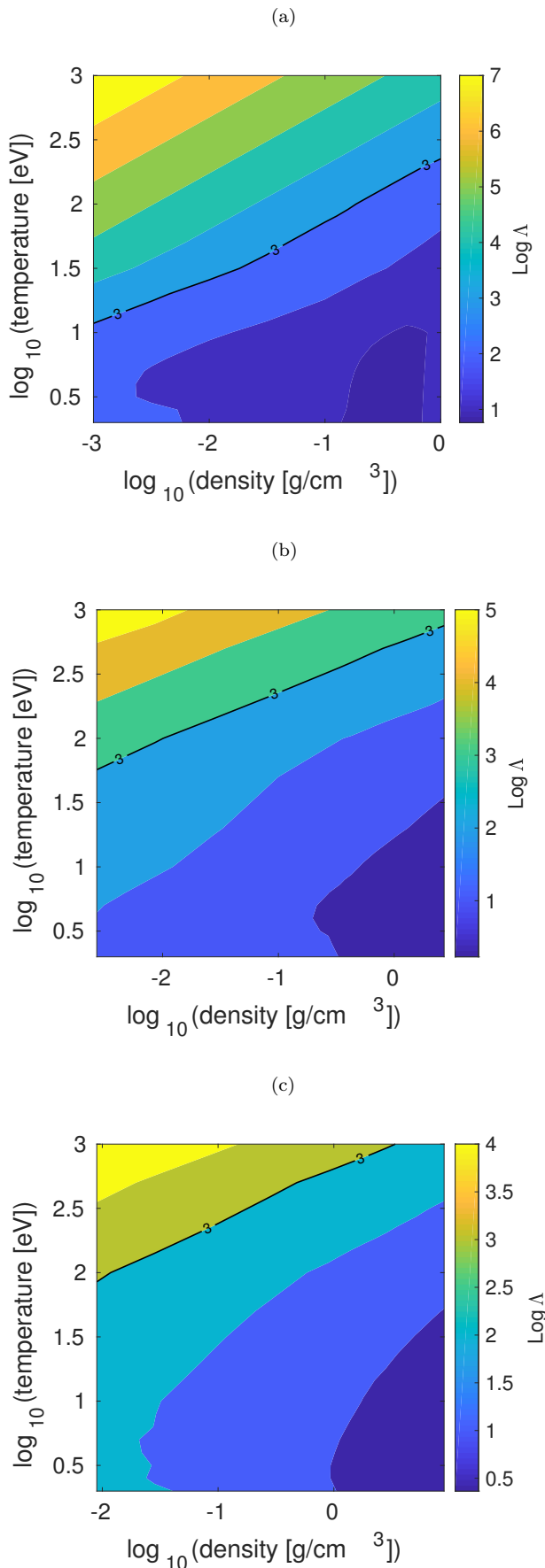


FIG. 8: Contour plot of  $\log \Lambda$  for (a) hydrogen, (b) aluminum and (c) copper.

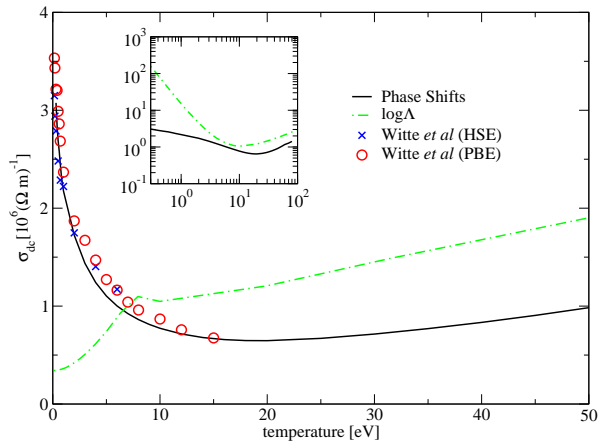


FIG. 9: (Color online) Electrical conductivity of solid density aluminum. The full quantum mechanical calculation (Phase Shifts) and the classical method ( $\log \Lambda$ ) are compared to Kubo-Greenwood DFT-MD calculations of Witte *et al* [33]. The inset compares the fully quantum mechanical calculations to  $\log \Lambda$  results that do not use degeneracy corrections (see text).

to? Of course this depends on the material. In figure 8 contour plots of  $\log \Lambda$  versus temperature and density for hydrogen, aluminum and copper are shown. Clearly, as  $Z$  increases the region where  $\log \Lambda > 3$  shrinks, leaving only the high temperature, low density region. This region corresponds to the least degenerate plasma. Assuming an accuracy better than  $\pm 10\%$  is required for the DC conductivity, it is clear that the classical  $\log \Lambda$  results cover only a limited region of phase space, and the more accurate quantum approach must be used elsewhere.

As a final example to highlight this result, in figure 9 these models are compared to recent Kubo-Greenwood, DFT-MD simulation results [33] for solid density aluminum in the relatively low temperature regime. There are two sets of DFT-MD results corresponding to two different exchange and correlation potentials (PBE [34] and HSE [35]). The full quantum model agrees well with both sets of DFT-MD results. The agreement is not perfect but given the very different models it is very encouraging. In contrast the classical  $\log \Lambda$  result is qualitatively and quantitatively different. The change in behavior at  $\sim 8$  eV is due to the degeneracy corrections to the impact parameters. In the inset the result without these degeneracy corrections is shown, i.e. replacing equations (5) and (9)

$$\lambda_{DH}^{-2} = \frac{4\pi\bar{n}_e^0 e^2}{kT} + \frac{4\pi\bar{Z}^2 n_i^0 e^2}{kT} \quad (16)$$

and

$$\bar{v} = v_{rms} \quad (17)$$

Clearly, the degeneracy corrections do not yield accurate

conductivities and they provide a only a marginal improvement over the uncorrected impact parameters.

#### IV. CONCLUSIONS

A comparison of a quantum mechanical calculation for a realistic scattering potential to the classical  $\log \Lambda$  approach has revealed that the classical method is accuracy to  $\pm 10\%$  when  $\log \Lambda > 3$ . The classical method requires an ionization model and it was found that the widely used and inexpensive Thomas-Fermi-Cell (TFC) model [18] provides a sufficiently accurate ionization estimate where the  $\log \Lambda$  method is also accurate (i.e.  $\log \Lambda > 3$ ).

The thermodynamic regime which corresponds to  $\log \Lambda > 3$  depends strongly on the material. For increasing  $Z$  this regime moves to higher temperatures and lower densities. This implies that, if accuracies in electrical conductivity better than  $\pm 10\%$  are required, then the  $\log \Lambda$  method can only be used if  $\log \Lambda > 3$  and in general one must generate tables on data that can later be interpolated.

It is noted that other transport coefficients such as thermal conductivity, electron-ion temperature relax-

ation and stopping power also rely on the electron momentum transport cross section. Hence, while this work is limited to electrical conductivity, the conclusions are expected to translate to these other processes, though perhaps in a non-trivial way.

This study is limited in a number of ways; only electron-ion collisions have been considered, the effect of electron-electron collisions on the conductivity has not been studied here; the plasma has been assumed to be made up of an ensemble of identical pseudo-atoms that all have the same average ionization; and only pure plasmas have been considered, i.e. mixtures are not considered. However, none of these limitations affect the conclusions since they are common to both the classical and quantum approaches. They do, however, point to future directions for improvement and testing.

#### Acknowledgments

The author thanks B. Witte and S. X. Hu for providing their DFT-MD results. This work was performed under the auspices of the United States Department of Energy under contract DE-AC52-06NA25396.

- 
- [1] Robert S. Cohen, Lyman Spitzer, and Paul McR. Routly. The electrical conductivity of an ionized gas. *Phys. Rev.*, 80:230–238, Oct 1950.
  - [2] J. Daligault and S. Gupta. Electron-ion scattering in dense multi-component plasmas: Application to the outer crust of an accreting neutron star. *The Astrophysical Journal*, 703(1):994, 2009.
  - [3] Alexander Y. Potekhin, D. A. Baiko, Pawel Haensel, and Dmitry G. Yakovlev. Transport properties of degenerate electrons in neutron star envelopes and white dwarf cores. *Astronomy and Astrophysics*, 346:345–353, 1999.
  - [4] John Lindl. Development of the indirect-drive approach to inertial confinement fusion and the target physics basis for ignition and gain. *Physics of plasmas*, 2(11):3933–4024, 1995.
  - [5] S. X. Hu, L. A. Collins, T. R. Boehly, J. D. Kress, V. N. Goncharov, and S. Skupsky. First-principles thermal conductivity of warm-dense deuterium plasmas for inertial confinement fusion applications. *Phys. Rev. E*, 89:043105, Apr 2014.
  - [6] D. O. Gericke, M. S. Murillo, and M. Schlanges. Dense plasma temperature equilibration in the binary collision approximation. *Phys. Rev. E*, 65:036418, Mar 2002.
  - [7] S. K. Kodanova, M. K. Issanova, S. M. Amirov, T. S. Ramazanov, A. Tikhonov, and Zh. A. Moldabekov. Relaxation of non-isothermal hot dense plasma parameters. *Matter and Radiation at Extremes*, 3(1):40–49, 2018.
  - [8] Lorin X. Benedict, Michael P. Surh, Liam G. Stanton, Christian R. Scullard, Alfredo A. Correa, John I. Castor, Frank R. Graziani, Lee A. Collins, Ondřej Čertík, Joel D. Kress, et al. Molecular dynamics studies of electron-ion temperature equilibration in hydrogen plasmas within the coupled-mode regime. *Physical Review E*, 95(4):043202, 2017.
  - [9] Jérôme Daligault and Guy Dimonte. Correlation effects on the temperature-relaxation rates in dense plasmas. *Physical Review E*, 79(5):056403, 2009.
  - [10] Günter Zwirnagel, Christian Toepffer, and Paul-Gerhard Reinhard. Stopping of heavy ions in plasmas at strong coupling. *Physics reports*, 309(3):117–208, 1999.
  - [11] K. Morawetz and G. Röpke. Stopping power in nonideal and strongly coupled plasmas. *Phys. Rev. E*, 54:4134–4146, Oct 1996.
  - [12] Yim T. Lee and R. M. More. An electron conductivity model for dense plasmas. *The Physics of fluids*, 27(5):1273–1286, 1984.
  - [13] W. A. Stygar, G. A. Gerdin, and D. L. Fehl. Analytic electrical-conductivity tensor of a nondegenerate lorentz plasma. *Physical Review E*, 66(4):046417, 2002.
  - [14] A. V. Filippov, A. N. Starostin, and V. K. Gryaznov. Coulomb logarithm in nonideal and degenerate plasmas. *Journal of Experimental and Theoretical Physics*, 126(3):430–439, 2018.
  - [15] C.E. Starrett. Potential of mean force for electrical conductivity of dense plasmas. *High Energy Density Physics*, 25:8 – 14, 2017.
  - [16] N David Mermin. Thermal properties of the inhomogeneous electron gas. *Physical Review*, 137(5A):A1441, 1965.
  - [17] Junzo Chihara. Unified description of metallic and neutral liquids and plasmas. *Journal of Physics: Condensed Matter*, 3(44):8715, 1991.
  - [18] R. P. Feynman, N. Metropolis, and E. Teller. Equations of state of elements based on the generalized fermi-thomas theory. *Phys. Rev.*, 75:1561–1573, May 1949.
  - [19] Lyman Spitzer, Jr. and Harlow Shapley. The stability

- of isolated clusters. *Monthly Notices of the Royal Astronomical Society*, 100(5):396–413, 1940.
- [20] S. V. Temko. On the derivation of the fokker-planck equation for a plasma. *Journal of Experimental and Theoretical Physics*, 6:898, 1957.
- [21] P. L. Bhatnagar, E. P. Gross, and M. Krook. A model for collision processes in gases. i. small amplitude processes in charged and neutral one-component systems. *Phys. Rev.*, 94:511–525, May 1954.
- [22] Nicholas A. Krall and Alvin W. Trivelpiece. *Principles of Plasma Physics*. New York, :McGraw-Hill, 1973.
- [23] H. Reinholz, G. Röpke, S. Rosmej, and R. Redmer. Conductivity of warm dense matter including electron-electron collisions. *Physical Review E*, 91(4):043105, 2015.
- [24] Michael P. Desjarlais, Christian R. Scullard, Lorin X. Benedict, Heather D. Whitley, and Ronald Redmer. Density-functional calculations of transport properties in the nondegenerate limit and the role of electron-electron scattering. *Phys. Rev. E*, 95:033203, Mar 2017.
- [25] C. E. Starrett and D. Saumon. Electronic and ionic structures of warm and hot dense matter. *Phys. Rev. E*, 87:013104, Jan 2013.
- [26] C.E. Starrett and D. Saumon. A simple method for determining the ionic structure of warm dense matter. *High Energy Density Physics*, 10:35 – 42, 2014.
- [27] AN Souza, DJ Perkins, CE Starrett, D Saumon, and SB Hansen. Predictions of x-ray scattering spectra for warm dense matter. *Physical Review E*, 89(2):023108, 2014.
- [28] C. E. Starrett and D. Saumon. Models of the elastic x-ray scattering feature for warm dense matter. *Phys. Rev. E*, 92:033101, 2015.
- [29] Jérôme Daligault, Scott D. Baalrud, Charles E. Starrett, Didier Saumon, and Travis Sjostrom. Ionic transport coefficients of dense plasmas without molecular dynamics. *Physical review letters*, 116(7):075002, 2016.
- [30] Simon Groth, Tobias Dornheim, Travis Sjostrom, Fionn D. Malone, W. M. C. Foulkes, and Michael Bonitz. Ab initio exchange-correlation free energy of the uniform electron gas at warm dense matter conditions. *Phys. Rev. Lett.*, 119:135001, Sep 2017.
- [31] M.P. Desjarlais. Practical improvements to the lee-more conductivity near the metal-insulator transition. *Contributions to Plasma Physics*, 41(2-3):267–270, 2001.
- [32] Michael S. Murillo, Jon Weisheit, Stephanie B. Hansen, and M. W. C. Dharma-Wardana. Partial ionization in dense plasmas: Comparisons among average-atom density functional models. *Physical Review E*, 87(6):063113, 2013.
- [33] B. B. L. Witte, P. Sperling, M. French, V. Recoules, S. H. Glenzer, and R. Redmer. Observations of non-linear plasmon damping in dense plasmas. *Physics of Plasmas*, 25(5):056901, 2018.
- [34] John P. Perdew, Kieron Burke, and Matthias Ernzerhof. Generalized gradient approximation made simple. *Physical review letters*, 77(18):3865, 1996.
- [35] Jochen Heyd, Gustavo E. Scuseria, and Matthias Ernzerhof. Hybrid functionals based on a screened coulomb potential. *The Journal of Chemical Physics*, 118(18):8207–8215, 2003.